Solid-State Electronics 73 (2012) 60–63

Contents lists available at SciVerse ScienceDirect

Solid-State Electronics

journal homepage: www.elsevier.com/locate/sse

Highly uniform low-power resistive memory using nitrogen-doped tantalum pentoxide

C.H. Cheng [a,*], P.C. Chen [b], Y.H. Wu [b], M.J. Wu [c], F.S. Yeh [a], Albert Chin [d]

[a] Department of Electronics Engineering and Institute of Electronics Engineering, National Tsing-Hua Univ., Hsinchu, Taiwan, ROC
[b] Department of Engineering and System Science, National Tsing-Hua Univ., Hsinchu, Taiwan, ROC
[c] Department of Mechanical Eng., National Chiao-Tung Univ., Hsinchu, Taiwan, ROC
[d] Department of Electronics Eng., National Chiao-Tung Univ., Hsinchu, Taiwan, ROC

ARTICLE INFO

Article history:
Received 19 August 2011
Received in revised form 4 March 2012
Accepted 8 March 2012
Available online 23 April 2012

The review of this paper was arranged by Prof. S. Cristoloveanu

Keywords:
Hopping conduction
Uniformity
TaON
RRAM
GeO_x

ABSTRACT

Highly uniform current distributions of high resistance state (HRS) and low resistance state (LRS), low 0.6 pJ switching energy, fast 30 ns switching speed, and good 10^6 cycling endurance are achieved in $Ni/GeO_x/Ta_2O_{5-y}N_y/TaN$ resistive random access memory (RRAM) devices. Such good performance is attributed to nitrogen-related acceptor level in $Ta_2O_{5-y}N_y$ for better hopping conduction, which leads to forming-free resistive switching and low self-compliance switching currents.

© 2012 Elsevier Ltd. All rights reserved.

The endurance degradation of Flash memory [1–3] at highly scaled sub-25 nm cell size is the fundamental physical limitation as listed in *International Technology Roadmap for Semiconductors* (*ITRS*) [1]. Therefore, new non-volatile memory (NVM) devices should be developed. Among various NVM devices, the resistive random access memory (RRAM) [4–15] has the simpler structure, faster switching speed, and better embedded memory integration beyond the Flash memory. However, the poor switching uniformity, high set/reset currents, large compliance currents with large size transistor, and low endurance are the difficult challenges for RRAM devices. To address these issues, we previously used the hopping conduction [16] to reach low switching current RRAMs [12–14]. The hopping conduction provides a large internal resistance to reach low self-compliance set/reset currents with unique negative temperature coefficient (TC), which is quite different from the large switching currents and the positive TC in conventional metal–oxide (MO) RRAM by metallic filament conduction [4]. Similar low switching power RRAM, using hopping conduction with negative TC, was also demonstrated by Samsung [15]. However, the switching current distribution needs to be improved to reach the production-level requirement of low tail bits.

In this paper, we report an ultra-low 0.6 pJ switching energy GeO/TaON RRAM with much tighter distribution and more stable endurance to 10^6 cycles. Such excellent performance is attributed to low self-compliance set/reset currents with the hopping conduction via nitrogen defects which is different to reported $Pt/TaO_x/Pt$ RRAM [11] with a large-size transistor to drive high current compliance.

The RRAM devices were integrated into VLSI backend with a 200-nm SiO_2 on a Si substrate. Then 100 nm TaN was deposited by physical vapor deposition (PVD). After patterning the TaN electrode, the 36-nm-thick $Ta_2O_{5-y}N_y$ dielectric was deposited on $TaN/SiO_2/Si$ followed by the optimized annealed condition of 400 °C for 15 min under oxygen ambient. The $Ta_2O_{5-y}N_y$ film remained amorphous phase after annealing which has been examined by X-ray diffraction (XRD). The control Ta_2O_5 layer was also deposited for performance comparison. After that, a 7.5-nm-thick GeO_x was deposited to form the stacked $GeO_x/Ta_2O_{5-y}N_y$ dielectric. Finally, a 50-nm-thick Ni was deposited and patterned as top electrode by a metal mask with an area of 11,300 μm^2. The fabricated devices were characterized by capacitance–voltage (*C–V*), current–voltage (*I–V*), switching speed, and endurance measurements using an Agilent 4284 LCR meter, 4156 semiconductor parameter analyzer, 81110 pulse generator and oscilloscope.

Fig. 1a shows the swept *I–V* curves of the $Ni/GeO_x/Ta_2O_{5-y}N_y/TaN$ and control $Ni/GeO_x/Ta_2O_5/TaN$ RRAM devices, and the swept

* Corresponding author.
E-mail address: raymondchengu@hotmail.com (C.H. Cheng).

0038-1101/$ - see front matter © 2012 Elsevier Ltd. All rights reserved.
http://dx.doi.org/10.1016/j.sse.2012.03.005

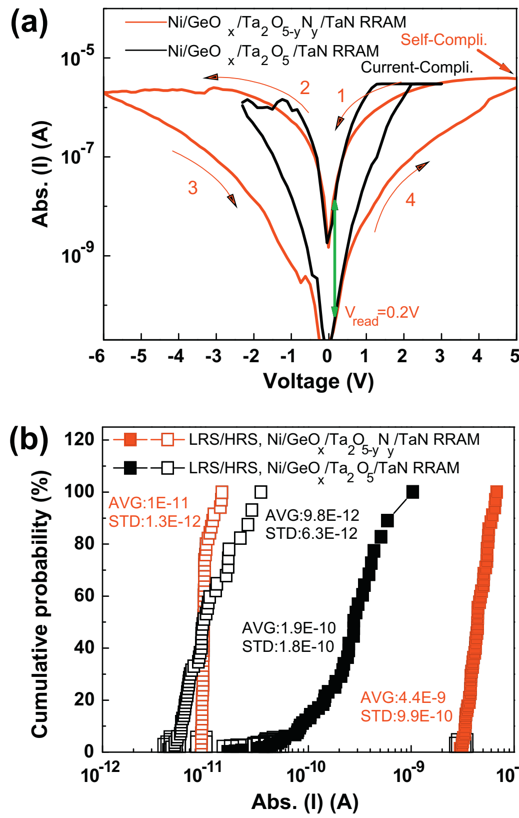

Fig. 1. (a) Swept I–V curves and (b) set/reset current distributions of Ni/GeO$_x$/Ta$_2$O$_{5-y}$N$_y$/TaN and control Ni/GeO$_x$/Ta$_2$O$_5$/TaN RRAM devices. The arrows indicate the bias sweeping directions.

directions were indicated by the arrows. The resistance changes from high resistance state (HRS) to low-resistance state (LRS) during set process, and changes from LRS to HRS during reset. The needed forming-free and self-compliance resistive switching characteristics are obtained in Ni/GeO$_x$/Ta$_2$O$_{5-y}$N$_y$/TaN RRAM device; however, the control Ni/GeO$_x$/Ta$_2$O$_5$/TaN device requires additional current-compliance to avoid breakdown during set/reset operations. The current-compliance will require a transistor to deliver and limit the set current, but the extra transistor consumes a larger area. The nitrogen-incorporated Ni/GeO$_x$/Ta$_2$O$_{5-y}$N$_y$/TaN RRAM device shows a resistance ratio >100 at 0.2 V read, a low set power of 19 μW (3.8 μA at 5 V) and reset power of 12 μW (−2 μA at −6 V). The low self-compliance currents during set/rest operation are related to the large internal resistance in nitrogen-doped RRAM device by hopping conduction [13]. To further investigate the nitrogen-doping effect, we have plotted the HRS/LRS current distributions in Fig. 1b. The control RRAM device, even with additional current-compliance, still exhibits wide LRS and HRS current distributions, which may be ascribed to random distribution of oxygen vacancies in Ta$_2$O$_5$ dielectric. In sharp contrast, highly uniform LRS and HRS currents and >100 resistance ratio are found in the nitrogen-doped RRAM device that is even better than published GeO/HfON RRAM [13]. The excellent switching uniformity is linked to the low power operation of forming-free resistive switching and low self-compliance set/reset currents, which have less stress to the dielectric of metal–insulator–metal (MIM) RRAM devices. This is significantly better than conventional RRAM using metallic filament conduction.

To explore such uniform switching currents, the current conduction mechanism was analyzed. Fig. 2a shows the measured and simulated I–V characteristics at HRS and LRS, respectively.

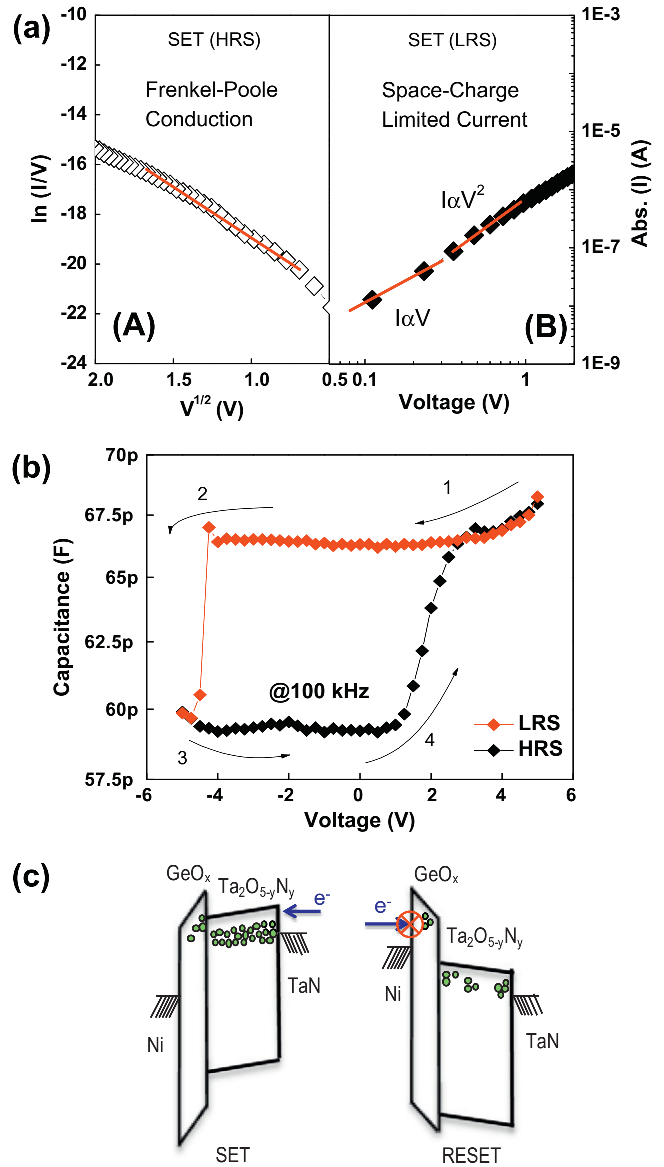

Fig. 2. (a) Measured and simulated HRS and LRS currents, (b) C–V curves at HRS and LRS and (c) the schematic energy band diagrams under set and reset conditions of Ni/GeO$_x$/Ta$_2$O$_{5-y}$N$_y$/TaN RRAM devices.

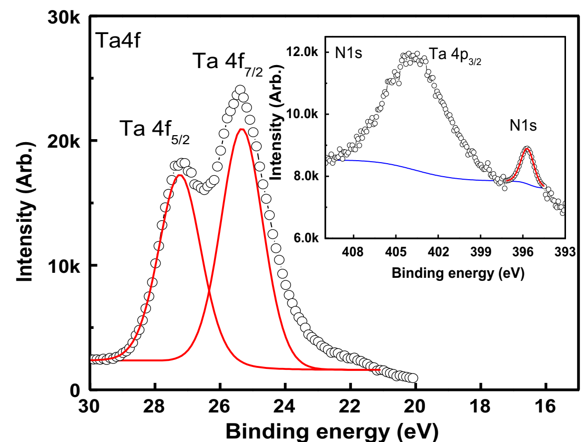

Fig. 3. The XPS spectra of Ta 4f and N 1s core level in Ta$_2$O$_{5-y}$N$_y$.

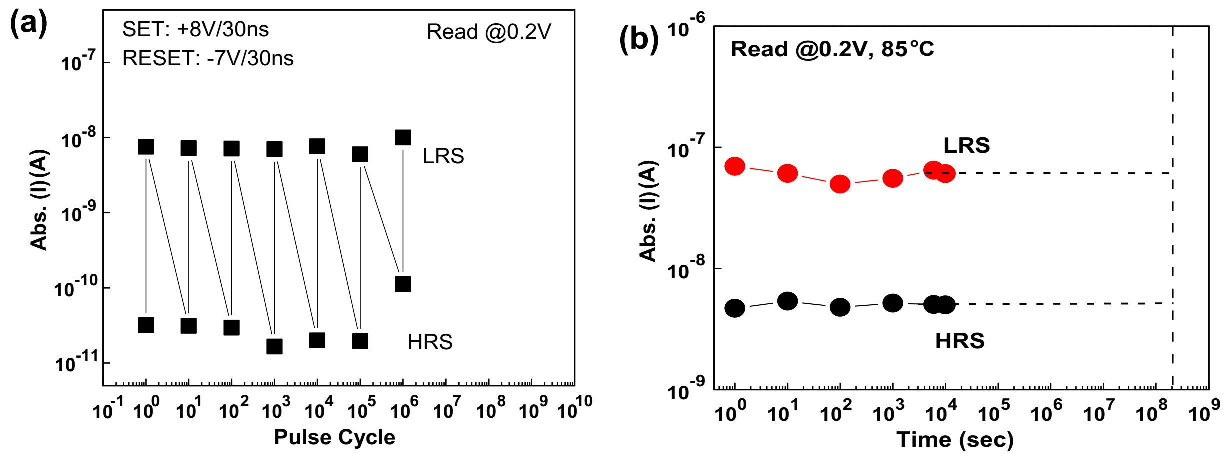

Fig. 4. (a) Endurance and (b) 85 °C retention characteristics of Ni/GeO_x/$Ta_2O_{5-y}N_y$/TaN RRAM devices.

Table 1
Comparison of device integrity data for various RRAM devices.

Dielectric	NiO [4]	TiO_2 [6]	CeO_x [8]	TaO_x [11]	GeO/HfON [13]	GeO/TaON (this work)
I_{SET}, @ V_{SET}	0.6 mA, 3.9 V	−1 mA, −1 V	10 mA, 0.8 V	−170 μA, −0.9 V	0.1 μA, 3 V	3.8 μA, 5 V
I_{RESET}, @V_{RESET}	5 mA, 1.4 V	1 mA, 1.1 V	−5 mA, −1.5 V	170 uA, 2 V	−0.3 nA, −1.8 V	−2 μA, −6 V
Self-compliance	No	No	No	No	Yes	Yes
HRS/LRS	~2 × 10^2	~10^2	~10^2	~10	9 × 10^2	10^2
Cycles, pulse	–	10^6, 5 ns	200 dc cycles	>10^9, 100 ns	10^6, 20 ns	10^6, 30 ns

The small HRS current is due to the Frenkel-Poole conduction [17] via the top Ni electrode. The current at LRS is governed by the space-charge-limited current (SCLC) via dielectric defects, for electrons injected from the bottom TaN electrode. Such resistive switching using hopping conduction[12–14] is supported by the *C–V* hysteresis loop shown in Fig. 2b. During set operation, the charged oxygen or nitrogen vacancies (V^{n+}) are formed for the hopping conduction by energetic electrons injected from bottom TaN electrode. This will create more dielectric charges (Q_d) in the MIM RRAM capacitor. During the reset, the electrons were injected from the top high work-function Ni electrode to neutralize charged vacancies and thereby break the hopping conduction pass [13]:

$$V^{n+} + ne^- \rightarrow V^{0*} \quad (1)$$

Here the V^{0*} is the neutralized vacancy state in the dielectric. Since the voltage differences for process 4 and 1, or 2 and 3 are the same, the extra larger Q_d is measurable by the higher capacitance. The above explanation and related mechanism are shown schematically in Fig. 2c. The hopping conduction also provides a large internal resistance [13] to reach a small self-compliance set current.

To investigate the role of nitrogen-doped RRAM, the chemical states of $Ta_2O_{5-y}N_y$ were examined by X-ray photoelectron spectroscopy (XPS). Fig. 3 shows the XPS spectra of Ta 4f and N 1s core level in $Ta_2O_{5-y}N_y$ dielectric. The measured Ta 4f7/2 and 5f/2 peaks were at 27.2 and 25.4 eV respectively, which are lower than those of reported Ta_2O_5 [18]. The shift of Ta 4f7/2 peak energy to lower binding energy is due to nitrogen incorporation caused charge shift from Ta^{5+} to Ta^{4+}. Furthermore, the peak of N 1s at 396.6 eV (N^{3-}) verifies the nitrogen-doping in $Ta_2O_{5-y}N_y$. The doped nitrogen forms an acceptor level at substitutional oxygen sites and lead to a charge shift from Ta^{5+} to Ta^{4+}, where the electrons can transport via nitrogen-related acceptor by hopping conduction [19,20].

The endurance measurement is an important test for RRAM to replace Flash memory. The endurance characteristics were measured under an over-stressed 8 V set pulse and −7 V reset pulse at a switching speed of 30 ns applied to RRAM device. Fig. 4a shows the measured endurance characteristics, where stable cycled endurance with more than 2 orders LRS/HRS resistance ratio is obtained up to 10^6 cycles. The stable cycled HRS and LRS currents and long endurance in this RRAM device are ascribed to the low self-compliance switching currents and hopping conduction via nitrogen defects. Fig. 4b shows the retention characteristics at elevated temperature of 85 °C. Stable HRS/LRS memory window is measured with retention time to 10^4 sec. Table 1 compares various RRAM devices. Our device has merits of low self-compliance set/reset currents, fast 30 ns switching time and excellent 10^6 cycling endurance in addition to a tight current distribution.

In summary, the nitrogen-doped Ni/GeO_x/$Ta_2O_{5-y}N_y$/TaN RRAM shows low 0.6 pJ switching energy, fast 30 ns switching speed, and good 10^6 cycling endurance, which is ascribed to nitrogen-related acceptor level in $Ta_2O_{5-y}N_y$ for better hopping conduction, forming-free resistive switching, and low self-compliance currents.

Acknowledgment

The paper publication was supported by National Science Council of Taiwan.

References

[1] International Technology Roadmap for Semiconductors (ITRS); 2009 <http://www.itrs.net> [Online].
[2] Lin SH, Chin Albert, Yeh FS, McAlister SP. In: Tech. dig. – int. electron devices meet; 2008. p. 843.
[3] Lai CH, Chin Albert, Kao HL, Chen KM, Hong M, Kwo J, et al. Sympos VLSI Technol 2006:54.
[4] Russo U, Ielmini D, Cagli C, Lacaita AL, Spiga S, Wiemer C, et al. In: Tech Dig – Int Electron Devices Meet; 2007. p. 775.
[5] Waser R, Aono M. Nature Mater 2007;6:833.
[6] Yoshida C, Tsunoda K, Noshiro H, Sugiyama Y. Appl Phys Lett 2007;91:223510.

[7] Xu N, Liu L, Sun X, Liu X, Han D, Wang Y, et al. Appl Phys Lett 2008;92: 232112.
[8] Sun X, Sun B, Liu L, Xu N, Liu X, Han R, et al. IEEE Electron Device Lett 2009;30:334.
[9] Cagli C, Nardi F, Ielmini D. IEEE Trans Electron Device 2009;56:1712.
[10] Sun B, Liu YX, Liu LF, Xu N, Wang Y, Liu XY, et al. Appl Phys Lett 2009;105:061630.
[11] Wei Z, Kanzawa Y, Arita K, Katoh Y, Kawai K, Muraoka S, et al. In: Tech dig – int electron devices meet; 2008. p. 1.
[12] Cheng CH, Chin Albert, Yeh YS. Appl Phys Lett 2011;98:052905.
[13] Cheng CH, Chin Albert, Yeh FS. In: Tech Dig – Int Electron Devices Meet; 2010. p. 448.
[14] Cheng CH, Chin Albert, Yeh FS. Adv Mater 2010;23:902.
[15] Kim MJ, Baek IG, Ha YH, Baik SJ, Kim JH, Seong DJ, et al. In: Tech Dig – Int Electron Devices Meet; 2010. 444.
[16] Chin A, Lee K, Lin BC, Horng S. Appl Phys Lett 1996;69:653.
[17] Yeh CC, Ma TP, Ramaswamy N, Rocklein N, Gealy D, Graettinger T, et al. Appl Phys Lett 2007;91:113521.
[18] Nie HB, Xu SY, Wang SJ, You LP, Yang Z, Ong CK, et al. Appl Phys A 2001;73:229.
[19] Morikawa T, Saeki S, Suzuki T, Kajino T, Motohiro T. Appl Phys Lett 2010;96:142111.
[20] Majumdar S, Banerji P. J Appl Phys 2010;107:063702.